

DFG-Schwerpunktprogramm 1324

„Extraktion quantifizierbarer Information aus komplexen Systemen“

Compactly Supported Shearlets are Optimally Sparse

G. Kutyniok, W.-Q Lim

Preprint 38



Edited by

AG Numerik/Optimierung
Fachbereich 12 - Mathematik und Informatik
Philipps-Universität Marburg
Hans-Meerwein-Str.
35032 Marburg

DFG-Schwerpunktprogramm 1324

„Extraktion quantifizierbarer Information aus komplexen Systemen“

Compactly Supported Shearlets are Optimally Sparse

G. Kutyniok, W.-Q Lim

Preprint 38



The consecutive numbering of the publications is determined by their chronological order.

The aim of this preprint series is to make new research rapidly available for scientific discussion. Therefore, the responsibility for the contents is solely due to the authors. The publications will be distributed by the authors.

COMPACTLY SUPPORTED SHEARLETS ARE OPTIMALLY SPARSE

GITTA KUTYNIOK* AND WANG-Q LIM †

Abstract. Cartoon-like images, i.e., C^2 functions which are smooth apart from a C^2 discontinuity curve, have by now become a standard model for measuring sparse (non-linear) approximation properties of directional representation systems. It was already shown that curvelets, contourlets, as well as shearlets do exhibit (almost) optimally sparse approximation within this model. However, all those results are only applicable to band-limited generators, whereas, in particular, spatially compactly supported generators are of uttermost importance for applications.

In this paper, we now present the first complete proof of (almost) optimally sparse approximations of cartoon-like images by using a particular class of directional representation systems, which indeed consists of compactly supported elements. This class will be chosen as a subset of shearlet frames – not necessarily required to be tight – with shearlet generators having compact support and satisfying some weak moment conditions.

Key words. Curvilinear discontinuities, edges, nonlinear approximation, optimal sparsity, shearlets, thresholding, wavelets

AMS subject classifications. Primary 42C40; Secondary 42C15, 65T60, 65T99, 94A08

1. Introduction. In computer vision, edges were detected as those features governing an image while separating smooth regions in between. About 10 years ago, mathematicians started to design models of images incorporating those findings aiming at designing representation systems which – in such a model – are capable of resolving edges in an optimally sparse way. However, customarily, at that time an image was viewed as an element of a compact subset of L_p characterized by a given Besov regularity with the Kolmogorov entropy of such sets identifying lower bounds for the distortion rates of encoding-decoding pairs in this model. Although wavelets could be shown to behave optimally [2] as an encoding methodology, Besov models are clearly deficient since edges are not adequately captured. This initiated the introduction of a different model, called cartoon-like model (see [5, 19, 1]), which revealed the suboptimal treatment of edges by wavelets.

The introduction of tight curvelet frames in 2004 by Candés and Donoho [1], which provably provide (almost) optimally sparse approximations within such a cartoon-like model can be considered a milestone in applied harmonic analysis. One year later, contourlets were introduced by Do and Vetterli [4] which similarly derived (almost) optimal approximation rates. In the same year, *shearlets* were developed by Labate, Weiss, and the authors in [17] as the first directional representation system with allows a unified treatment of the continuum and digital world similar to wavelets, while also providing (almost) optimally sparse approximations within such a cartoon-like model [11].

In most applications, spatial localization of the analyzing elements of an encoding system is of uttermost importance both for a precise detection of geometric features as

*Institute of Mathematics, University of Osnabrück, 49069 Osnabrück, Germany (kutyniok@uni-osnabrueck.de).

†Institute of Mathematics, University of Osnabrück, 49069 Osnabrück, Germany (wlim@uni-osnabrueck.de).

G.K. and W.-Q L. would like to thank Wolfgang Dahmen, David Donoho, Chunyan Huang, Demetrio Labate, Christoph Schwab, and Gerrit Welper for various discussions on related topics. G.K. and W.-Q L. acknowledge support from DFG Grant SPP-1324, KU 1446/13-1.

well as for a fast decomposition algorithm. However, none of the previously mentioned results cover this situation. In fact, the proofs which were provided do by no means extend to this crucial setting.

In this paper, we now present the first complete proof of (almost) optimally sparse approximations of cartoon-like images by using a particular class of directional representation systems, which indeed consist of compactly supported elements. This class will be chosen as a subset of shearlet frames – not necessarily required to be tight – with shearlet generators having compact support and satisfying some weak moment conditions. Interestingly, our proof is very different from all previous ones caused by the extensive exploration of the compact support of the shearlet generators and the lack of directional vanishing moments.

1.1. A Suitable Model for Images: Cartoon-Like Images. Intuitively, cartoons are smooth image parts separated from other areas by an edge. After a series of initial models [5, 19], the first complete model of cartoons has been introduced in [1], and this is what we intend to use also here. The basic idea is to choose a closed boundary curve and then fill the interior and exterior part with C^2 functions (see Figure 1.1).

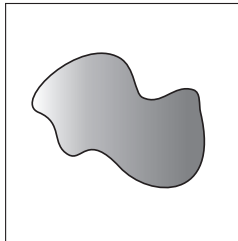


FIG. 1.1. Example of a cartoon-like image.

Let us now be more precise, and introduce $STAR^2(\nu)$, a class of indicator functions of sets B with C^2 boundaries ∂B and curvature bounded by ν , as well as $\mathcal{E}^2(\nu)$, a class of cartoon-like images. For this, in polar coordinates, we let $\rho(\theta) \rightarrow [0, 1]^2$ be a radius function and define the set B by

$$B = \{x \in \mathbb{R}^2 : |x| \leq \rho(\theta), x = (|x|, \theta) \text{ in polar coordinates}\}.$$

In particular, the boundary ∂B of B is given by the curve

$$\beta(\theta) = \begin{pmatrix} \rho(\theta) \cos(\theta) \\ \rho(\theta) \sin(\theta) \end{pmatrix}, \quad (1.1)$$

and the class of boundaries of interest to us are defined by

$$\sup |\rho''(\theta)| \leq \nu, \quad \rho \leq \rho_0 < 1. \quad (1.2)$$

The following definition now introduces the notions $STAR^2(\nu)$ and $\mathcal{E}^2(\nu)$ from [1]. As it is custom, we denote the space of continuously differentiable functions on $[0, 1]^2$ with compact support by $C_0([0, 1]^2)$.

DEFINITION 1.1. For $\nu > 0$, the set $STAR^2(\nu)$ is defined to be the set of all $B \subset [0, 1]^2$ such that B is a translate of a set obeying (1.1) and (1.2). Further, $\mathcal{E}^2(\nu)$ denotes the set of functions $f \in L^2(\mathbb{R}^2)$ of the form

$$f = f_0 + f_1 \chi_B,$$

where $f_0, f_1 \in C_0^2([0, 1]^2)$, $B \in STAR^2(\nu)$, and $\|f\|_{C^2} = \sum_{|\alpha| \leq 2} \|D^\alpha f\|_\infty \leq 1$.

1.2. Optimal Sparsity of a Directional Representation System. The ‘quality’ of the performance of a (directional) representation system with respect to cartoon-like images is typically measured by taking a non-linear approximation viewpoint. More precisely, given a cartoon-like image $f \in \mathcal{E}^2(\nu)$ and a (directional) representation system $(\sigma_i)_{i \in I}$ which forms an orthonormal basis, the chosen measure is the asymptotic behavior of the best N -term (non-linear) approximation error in L^2 norm in the number of terms N , i.e.,

$$\|f - f_N\|_2^2 = \left\| f - \sum_{i \in I_N} \langle f, \sigma_i \rangle \sigma_i \right\|_2^2 \quad \text{as } N \rightarrow \infty,$$

where $(\langle f, \sigma_i \rangle)_{i \in I_N}$ are the N largest coefficients $\langle f, \sigma_i \rangle$ in magnitude. Wavelet bases exhibit the approximation rate

$$\|f - f_N\|_2^2 \leq C \cdot N^{-1} \quad \text{as } N \rightarrow \infty.$$

However, Donoho proved in [6] that the optimal rate which can be achieved under some restrictions on the representation system as well as on the selection procedure of the approximating coefficients is

$$\|f - f_N\|_2^2 \leq C \cdot N^{-2} \quad \text{as } N \rightarrow \infty.$$

It was a breakthrough in 2004, when Candés and Donoho introduced the tight curvelet frame in [1] and proved that this system indeed does satisfy

$$\|f - f_N\|_2^2 \leq C \cdot N^{-2} \cdot (\log N)^3 \quad \text{as } N \rightarrow \infty,$$

where again the approximation f_N was generated by the N largest coefficients in magnitude. Although the optimal rate is not completely achieved, the log-factor is typically considered negligible compared to the N^{-2} -factor, wherefore the term ‘almost optimal’ has been adopted into the language. This result is even more surprising taking into account that in case of a tight frame the approximation by the N largest coefficients in magnitude does not even always yield the *best* N -term approximation.

1.3. (Compactly Supported) Shearlet Systems. The directional representation system of *shearlets* has recently emerged and rapidly gained attention due to the fact that – in contrast to other proposed directional representation systems – shearlets provide a unified treatment of the continuum and digital world similar to wavelets. We refer to, e.g., [9, 15] for the continuum theory, [16, 8, 18] for the digital theory, and [10, 7] for recent applications.

Shearlets are scaled according to a parabolic scaling law encoded in the *parabolic scaling matrices* A_{2^j} or \tilde{A}_{2^j} , $j \in \mathbb{Z}$, and exhibit directionality by parameterizing slope encoded in the *shear matrices* S_k , $k \in \mathbb{Z}$, defined by

$$A_{2^j} = \begin{pmatrix} 2^j & 0 \\ 0 & 2^{j/2} \end{pmatrix} \quad \text{or} \quad \tilde{A}_{2^j} = \begin{pmatrix} 2^{j/2} & 0 \\ 0 & 2^j \end{pmatrix}$$

and

$$S_k = \begin{pmatrix} 1 & -k \\ 0 & 1 \end{pmatrix},$$

respectively.

To ensure an (almost) equal treatment of the different slopes, which is evidently of significant importance for practical applications, we partition the frequency plane into the following four cones $\mathcal{C}_1 - \mathcal{C}_4$:

$$\mathcal{C}_\iota = \begin{cases} \{(\xi_1, \xi_2) \in \mathbb{R}^2 : \xi_1 \geq 1, |\xi_2/\xi_1| \geq 1\} & : \iota = 1, \\ \{(\xi_1, \xi_2) \in \mathbb{R}^2 : \xi_2 \geq 1, |\xi_1/\xi_2| \leq 1\} & : \iota = 2, \\ \{(\xi_1, \xi_2) \in \mathbb{R}^2 : \xi_1 \leq -1, |\xi_2/\xi_1| \geq 1\} & : \iota = 3, \\ \{(\xi_1, \xi_2) \in \mathbb{R}^2 : \xi_2 \leq -1, |\xi_1/\xi_2| \leq 1\} & : \iota = 4, \end{cases}$$

and a centered rectangle

$$\mathcal{R} = \{(\xi_1, \xi_2) \in \mathbb{R}^2 : \|(\xi_1, \xi_2)\|_\infty < 1\}.$$

For an illustration, we refer to Figure 1.2(a).



FIG. 1.2. (a) The cones $\mathcal{C}_1 - \mathcal{C}_4$ and the centered rectangle \mathcal{R} in frequency domain. (b) The tiling of the frequency domain induced by a (cone-adapted) shearlet system.

The rectangle \mathcal{R} corresponds to the low frequency content of a signal and is customarily represented by translations of some scaling function. Anisotropy comes into play when encoding the high frequency content of a signal which corresponds to the cones $\mathcal{C}_1 - \mathcal{C}_4$, where the cones \mathcal{C}_1 and \mathcal{C}_3 as well as \mathcal{C}_2 and \mathcal{C}_4 are treated separately as can be seen in the following

DEFINITION 1.2. For some sampling constant $c > 0$, the (cone-adapted) shearlet system $\mathcal{SH}(c; \phi, \psi, \tilde{\psi})$ generated by a scaling function $\phi \in L^2(\mathbb{R}^2)$ and shearlets $\psi, \tilde{\psi} \in L^2(\mathbb{R}^2)$ is defined by

$$\mathcal{SH}(c; \phi, \psi, \tilde{\psi}) = \Phi(c, \phi) \cup \Psi(c, \psi) \cup \tilde{\Psi}(c, \tilde{\psi}),$$

where

$$\Phi(c, \phi) = \{\phi_m = \phi(\cdot - cm) : m \in \mathbb{Z}^2\},$$

$$\Psi(c, \psi) = \{\psi_{j,k,m} = 2^{3j/4} \psi(S_k A_{2^j} \cdot -cm) : j \geq 0, |k| \leq \lceil 2^{j/2} \rceil, m \in \mathbb{Z}^2\},$$

and

$$\tilde{\Psi}(c, \tilde{\psi}) = \{\tilde{\psi}_{j,k,m} = 2^{3j/4} \tilde{\psi}(S_k^T \tilde{A}_{2^j} \cdot -cm) : j \geq 0, |k| \leq \lceil 2^{j/2} \rceil, m \in \mathbb{Z}^2\}.$$

The reader should keep in mind that although not indicated by the notation, the functions ϕ_m , $\psi_{j,k,m}$, and $\tilde{\psi}_{j,k,m}$ all depend on the sampling constant c . For the sake

of brevity, we will often write ψ_λ and $\tilde{\psi}_\lambda$, where $\lambda = (j, k, m)$ index scale, shear, and position. For later use, we further let Λ_j be the indexing sets of shearlets in $\Psi(c, \psi)$ and $\tilde{\Psi}(c, \tilde{\psi})$ at scale j , respectively, i.e.,

$$\Psi(c, \psi) = \{\psi_\lambda : \lambda \in \Lambda_j, j = 0, \dots, \infty\} \quad \text{and} \quad \tilde{\Psi}(c, \tilde{\psi}) = \{\tilde{\psi}_\lambda : \lambda \in \Lambda_j, j = 0, \dots, \infty\}.$$

Finally, we define

$$\Lambda = \bigcup_{j=0}^{\infty} \Lambda_j \quad \text{and} \quad \tilde{\Lambda} = \bigcup_{j=0}^{\infty} \tilde{\Lambda}_j.$$

The tiling of frequency domain induced by $\mathcal{SH}(c; \phi, \psi, \tilde{\psi})$ is illustrated in Figure 1.2(b). From this illustration, the anisotropic footprints of shearlets contained in $\Psi(c, \psi)$ and $\tilde{\Psi}(c, \tilde{\psi})$ can clearly be seen. However, the reader should notice that the tiling indicated here is based on the *essential support* and not the exact support of the analyzing elements, since our focus will be on shearlet systems associated with spatially compactly supported generators. The corresponding anisotropic footprints of shearlets *in spatial domain* are of size $2^{-j/2}$ times 2^{-j} . A beautiful intuitive extensive explanation of why it is conceivable that such a system – based on parabolic scaling – exhibits optimal sparse approximation of cartoon-like images, is provided in [1], and we would like to refer the reader to this paper. The main idea is to count the number of shearlets intersecting the discontinuity curves, which is ‘small’ compared to the number of such wavelets, due to their anisotropic footprints.

Certainly, we naturally ask the question when $\mathcal{SH}(c; \phi, \psi, \tilde{\psi})$ does form a frame for $L^2(\mathbb{R}^2)$. The wavelet literature provides various necessary and sufficient conditions for $\Phi(c, \phi)$ to form a frame for $L^2(\{f \in L^2(\mathbb{R}^2) : \text{supp}(\hat{f}) \subseteq \mathcal{R}\})$, also when ϕ is compactly supported in spatial domain. Although not that well-studied as wavelets yet, several answers are also known for the question when $\Psi(c, \psi)$ forms a frame for

$$L^2(\{f \in L^2(\mathbb{R}^2) : \text{supp}(\hat{f}) \subseteq \mathcal{C}_1 \cup \mathcal{C}_3\}),$$

and we refer to results in [9, 14, 3, 13]. Since $\Psi(c, \phi)$ and $\tilde{\Psi}(c, \tilde{\psi})$ are linked by a simple rotation of 90° , these results immediately provide conditions for $\tilde{\Psi}(c, \tilde{\psi})$ to constitute a frame for

$$L^2(\{f \in L^2(\mathbb{R}^2) : \text{supp}(\hat{f}) \subseteq \mathcal{C}_2 \cup \mathcal{C}_4\}).$$

Very recent results in [12] even focus specifically on the case of spatially compactly supported shearlets – of uttermost importance for application due to their superior localization. For instance, in [12], the following special class of compactly supported shearlet frames for $L^2(\mathbb{R}^2)$ was constructed: The generating shearlets ψ and $\tilde{\psi}$ were chosen separable, i.e., of the form $\psi_1(x_1) \cdot \psi_2(x_2)$ and $\psi_1(x_2) \cdot \psi_2(x_1)$, respectively, where ψ_1 is wavelet and ψ_2 a scaling function both associated with some carefully chosen low pass filter. Intriguingly, our main result in this paper (Theorem 1.3) proves as a corollary that this class of compactly supported shearlet frames provides (almost) optimally sparse approximations of cartoon-like images. We refer to [12] for the precise statement.

Combining those thoughts, we can attest that frame properties of $\mathcal{SH}(c; \phi, \psi, \tilde{\psi})$ including spatially compactly supported generators are already quite well studied.

1.4. Optimally Sparse Approximation of Cartoon-Like Images by Shearlets. The concept of optimally sparse approximation of cartoon-like images of general (directional) representation systems was already discussed in Section 1.2. However, the attentive reader will have realized that only the situation of tight frames was studied whereas here we intend to consider sparse approximations by arbitrary frames. Hence this situation deserves a careful commenting.

Let $\mathcal{SH}(c; \phi, \psi, \tilde{\psi})$ be a shearlet frame for $L^2(\mathbb{R}^2)$, which for illustrative purposes for a moment we denote by $\mathcal{SH}(c; \phi, \psi, \tilde{\psi}) = (\sigma_i)_{i \in I}$, say. Is it well-known that a frame is associated with a canonical dual frame, which in this case we want to call $(\tilde{\sigma}_i)_{i \in I}$. Then we define the N -term approximation f_N of a cartoon-like image $f \in \mathcal{E}^2(\nu)$ by the frame $\mathcal{SH}(c; \phi, \psi, \tilde{\psi})$ to be

$$f_N = \sum_{i \in I_N} \langle f, \sigma_i \rangle \tilde{\sigma}_i,$$

where $(\langle f, \sigma_i \rangle)_{i \in I_N}$ are the N largest coefficients $\langle f, \sigma_i \rangle$ in magnitude. As in the tight frame case, this procedure does not always yield the *best* N -term approximation, but surprisingly even with this ‘crude’ selection procedure – in the situation of spatially compactly supported generators – we can prove an (almost) optimally sparse approximation rate as our main result shows.

THEOREM 1.3. *Let $c > 0$, and let $\phi, \psi, \tilde{\psi} \in L^2(\mathbb{R}^2)$ be compactly supported. Suppose that, in addition, for all $\xi = (\xi_1, \xi_2) \in \mathbb{R}^2$, the shearlet ψ satisfies*

$$(i) \quad |\hat{\psi}(\xi)| \leq C_1 \cdot \min(1, |\xi_1|^\alpha) \cdot \min(1, |\xi_1|^{-\gamma}) \cdot \min(1, |\xi_2|^{-\gamma}) \text{ and}$$

$$(ii) \quad \left| \frac{\partial}{\partial \xi_2} \hat{\psi}(\xi) \right| \leq |h(\xi_1)| \cdot \left(1 + \frac{|\xi_2|}{|\xi_1|} \right)^{-\gamma},$$

where $\alpha > 5$, $\gamma \geq 4$, $h \in L^1(\mathbb{R})$, and C_1 is a constant, and suppose that the shearlet $\tilde{\psi}$ satisfies (i) and (ii) with the roles of ξ_1 and ξ_2 reversed. Further, suppose that $\mathcal{SH}(c; \phi, \psi, \tilde{\psi})$ forms a frame for $L^2(\mathbb{R}^2)$.

Then, for any $\nu > 0$, the shearlet frame $\mathcal{SH}(c; \phi, \psi, \tilde{\psi})$ provides (almost) optimally sparse approximations of functions $f \in \mathcal{E}^2(\nu)$, i.e., there exists some $C > 0$ such that

$$\|f - f_N\|_2^2 \leq C \cdot N^{-2} \cdot (\log N)^3 \quad \text{as } N \rightarrow \infty,$$

where f_N is the nonlinear N -term approximation obtained by choosing the N largest shearlet coefficients of f .

Condition (i) can be interpreted as both a condition ensuring (almost) separable behavior as well as a first order moment condition along the horizontal axis, hence enforcing directional selectivity. This condition ensures that the support of shearlets in frequency domain is essentially of the form indicated in Figure 1.2(b).

Condition (ii) combined with a modified version of condition (ii) by leaving out the derivative – this being implied by condition (i) – can be viewed as a generalization, thereby weakening, of a second order directional vanishing moment condition, which is crucial for having fast decay of the shearlet coefficients when the corresponding shearlet ψ_λ intersects the discontinuity curve. For the precise definition of directional vanishing moments, we refer to [4].

Notice also that intriguingly, the – the ‘true’ optimality destroying – log-factor has the *same* exponent as in the curvelet-, contourlet-, and shearlet-result on (almost) optimally sparse approximation.

1.5. Prior Work and Our Contribution. In 2004, Candés and Donoho [1] achieved a breakthrough when introducing tight curvelet frames, which provide (almost) optimally sparse approximations of cartoon-like images (functions in $\mathcal{E}^2(\nu)$). The main outline of their proof is to break $[0, 1]^2$ into smaller cubes and then separately analyze the curvelet coefficients essentially centered in the smooth part of the model and those essentially centered on the discontinuity curve. For both sets of coefficients their weak- $\ell_{2/3}$ norm is estimated; the estimate for the ‘non-smooth part’ also requiring the usage of the Radon transform.

A year later, Do and Vetterli [4] introduced contourlets and proved similar sparsity results for those. However, although their work includes contourlets with compact support, their construction is fully based on discrete filter banks so that directional selectivity is problematic. Because of this fact, infinite directional vanishing moments had to be artificially imposed in order to achieve (almost) optimal sparsity. However, this is impossible for any function with compact support to satisfy. Hence, similar to curvelets, optimal sparsity is only proven for *band-limited* contourlets.

In 2005, shearlets were introduced as the first directional representation system ensuring a unified treatment of the continuum and digital world by Labate, Weiss, and the authors in [17]. One year later, Labate and Guo proved (almost) optimally sparse approximations of cartoon-like images for the at that time customarily utilized shearlet frames [11], which are band-limited such as curvelets. The proof the authors provided follows the proof in [1] very closely step by step.

Concluding, although those pioneering studies deserve all our credit, these results are far from including the important class of directional representation systems consisting of compactly supported functions.

The main contribution of this paper is to provide the first complete proof of (almost) optimally sparse approximations of cartoon-like images using a directional representation system consisting of compactly supported functions. Our proof is indeed very different from all previous ones caused by the necessary extensive exploration of the compact support of the shearlet generators, the only similarity being the breaking of $[0, 1]^2$ into smaller cubes and the separate consideration of shearlet coefficients now being *exactly contained* – in contrast to being *essentially contained* for all other systems – in the smooth part and those which intersect the discontinuity curve. Previous results all require moment conditions along the direction of the discontinuity curve – thereby requiring vanishing moments along infinitely many directions asymptotically in scale –, which is trivially satisfied for band-limited generators. Intriguingly, a weaker version of directional vanishing moments, even only in one direction and the shearing taking care of the remaining directions, is sufficient for our analysis.

1.6. Outline. In Section 2, we present the overall structure of the proof, the results of the analysis of shearlet coefficients being contained in the smooth part and those which intersect the discontinuity curve, and – based on these results – state the proof of Theorem 1.3. The proofs of the results on the behavior of shearlet coefficients in the smooth and non-smooth part are then carried out in Sections 3 and 4, respectively.

2. Architecture of the Proof of Theorem 1.3. We now detail the general structure of the proof of Theorem 1.3, starting by introducing useful notions and explaining the blocking into smaller boxes and splitting into the smooth and non-smooth part. Then the main results concerning the analysis of shearlet coefficients being entirely contained in the smooth part and those intersecting the discontinuity

curve will be presented followed by the proof of Theorem 1.3 based on those.

2.1. General Organization. Let now $\mathcal{SH}(c; \phi, \psi, \tilde{\psi})$ satisfy the hypotheses of Theorem 1.3, and let $f \in \mathcal{E}^2(\nu)$. Further, we let A denote the lower frame bound of $\mathcal{SH}(c; \phi, \psi, \tilde{\psi})$.

We first observe that, without loss of generality, we might assume the scaling index j to be sufficiently large, since f as well as all frame elements in the shearlet frame $\mathcal{SH}(c; \phi, \psi, \tilde{\psi})$ are compactly supported in spatial domain, hence a finite number does not contribute to the asymptotic estimate we aim for. In particular, this means that we do not need to consider frame elements from Φ . Also, we are allowed to restrict our analysis to shearlets $\psi_{j,k,m}$, since the frame elements $\tilde{\psi}_{j,k,m}$ can be handled in a similar way.

Our main concern will be to derive appropriate estimates for the shearlet coefficients $\{\langle f, \psi_\lambda \rangle : \lambda \in \Lambda\}$ of f . Letting $|\theta(f)|_n$ denote the n th largest shearlet coefficient $\langle f, \psi_\lambda \rangle$ in absolute value and exploring the frame property of $\mathcal{SH}(c; \phi, \psi, \tilde{\psi})$, we conclude that

$$\|f - f_N\|_2^2 \leq \frac{1}{A} \sum_{n>N} |\theta(f)|_n^2,$$

for any positive integer N . Thus, for the proof of Theorem 1.3, it suffices to show that

$$\sum_{n>N} |\theta(f)|_n^2 \leq C \cdot N^{-2} \cdot (\log N)^3 \quad \text{as } N \rightarrow \infty. \quad (2.1)$$

To derive the anticipated estimate in (2.1), for any shearlet ψ_λ , we will study two separate cases:

- *Case 1.* The compact support of the shearlet ψ_λ does not intersect the boundary of the set B , i.e., $\text{supp}(\psi_\lambda) \cap \partial B = \emptyset$.
- *Case 2.* The compact support of the shearlet ψ_λ does intersect the boundary of the set B , i.e., $\text{supp}(\psi_\lambda) \cap \partial B \neq \emptyset$.

Notice that this exact distinction is only possible due to the spatial compact support of all shearlets in the shearlet frame.

In the sequel – since we are concerned with an asymptotic estimate – for simplicity we will often simply use C as a constant although it might differ for each estimate. Also all the results in the sequel are independent on the sampling constant $c > 0$, wherefore we now fix it once and for all.

2.2. The Smooth and the Non-Smooth Part. To illustrate which conditions on ψ required by Theorem 1.3 are utilized for the decay estimates of the different cases, in this section we do not make any initial assumptions on ψ .

Let us start with the smooth part, which is the easier one to handle. Dealing with this part allows us to consider some $g \in C_0^2([0, 1]^2)$ and estimate its shearlet coefficients. This is done in the following proposition. Notice that the hypothesis on ψ of the following result is implied by condition (i) in Theorem 1.3.

PROPOSITION 2.1. *Let $g \in C_0^2([0, 1]^2)$, and let $\psi \in L^2(\mathbb{R}^2)$ be compactly supported and satisfy*

$$|\hat{\psi}(\xi)| \leq C_1 \cdot \min(1, |\xi_1|^\alpha) \cdot \min(1, |\xi_1|^{-\gamma}) \cdot \min(1, |\xi_2|^{-\gamma}) \quad \text{for all } \xi = (\xi_1, \xi_2) \in \mathbb{R}^2,$$

where $\gamma > 3$, $\alpha > \gamma + 2$, and C_1 is a constant. Then, there exists some $C > 0$ such that

$$\sum_{n>N} |\theta(g)|_n^2 \leq C \cdot N^{-2} \quad \text{as } N \rightarrow \infty.$$

Thus, in this case, optimal sparsity is achieved. The proof of this proposition is given in Section 3.

Next, we turn our attention to the non-smooth part, in particular, to estimating those shearlet coefficients whose spatial support intersects the discontinuity curve. For this, we first need to introduce some new notations. For any scale $j \geq 0$ and any grid point $p \in \mathbb{Z}^2$, we let $\mathcal{Q}_{j,p}$ denote the dyadic cube defined by

$$\mathcal{Q}_{j,p} = [-2^{-j/2}, 2^{-j/2}]^2 + 2^{-j/2}p.$$

Further, let \mathcal{Q}_j be the collection of those dyadic cubes $\mathcal{Q}_{j,p}$ which intersect ∂B , i.e.,

$$\mathcal{Q}_j = \{\mathcal{Q}_{j,p} : \mathcal{Q}_{j,p} \cap \partial B \neq \emptyset, p \in \mathbb{Z}^2\}.$$

Of interest to us is also the set of shearlet indices, which are associated with shearlets intersecting the discontinuity curve inside some $\mathcal{Q}_{j,p} \in \mathcal{Q}_j$, i.e., for $j \geq 0$ and $p \in \mathbb{Z}^2$ with $\mathcal{Q}_{j,p} \in \mathcal{Q}_j$, we will consider the index set

$$\Lambda_{j,p} = \{\lambda \in \Lambda_j : \text{supp}(\psi_\lambda) \cap \mathcal{Q}_{j,p} \cap \partial B \neq \emptyset\}.$$

Finally, for $j \geq 0$, $p \in \mathbb{Z}^2$, and $0 < \varepsilon < 1$, we define $\Lambda_{j,p}(\varepsilon)$ to be the index set of shearlets ψ_λ , $\lambda \in \Lambda_{j,p}$, such that the magnitude of the corresponding shearlet coefficient $\langle f, \psi_\lambda \rangle$ is larger than ε and the support of ψ_λ intersects $\mathcal{Q}_{j,p}$ at the j th scale, i.e.,

$$\Lambda_{j,p}(\varepsilon) = \{\lambda \in \Lambda_{j,p} : |\langle f, \psi_\lambda \rangle| > \varepsilon\},$$

and we define $\Lambda(\varepsilon)$ to be the index set for shearlets so that $|\langle f, \psi_\lambda \rangle| > \varepsilon$ across all scales j , i.e.,

$$\Lambda(\varepsilon) = \bigcup_{j,p} \Lambda_{j,p}(\varepsilon).$$

The expert reader will have noticed that in contrast to the proofs in [1] and [11], which also split the domain into smaller scale boxes, we do not apply a weight function to obtain a smooth partition of unity. In our case, this is not necessary due to the spatial compact support of the frame elements.

As mentioned at the beginning of this section, we may assume that j is sufficiently large. Given some scale $j \geq 0$ and position $p \in \mathbb{Z}^2$ for which the associated cube $\mathcal{Q}_{j,p}$ satisfies $\mathcal{Q}_{j,p} \in \mathcal{Q}_j$. Then the set

$$\mathcal{S}_{j,p} = \bigcup_{\lambda \in \Lambda_{j,p}} \text{supp}(\psi_\lambda)$$

is contained in a cubic window of size $C \cdot 2^{-j/2}$ by $C \cdot 2^{-j/2}$, hence is of asymptotically the same size as $\mathcal{Q}_{j,p}$. Thus, we are facing the following two cases (see also Figure 2.1):

- *Case 2a.* The edge curve ∂B can be parameterized by $(E(x_2), x_2)$ with $E \in C^2([0, 1])$ inside $\mathcal{S}_{j,p}$ such that, for any $\lambda \in \Lambda_{j,p}$, there exists some $\hat{x} = (\hat{x}_1, \hat{x}_2) \in \mathcal{Q}_{j,p} \cap \text{supp}(\psi_\lambda) \cap \partial B$ satisfying $|E'(\hat{x}_2)| < \infty$.
- *Case 2b.* The edge curve ∂B can be parameterized by $(x_1, E(x_1))$ with $E \in C^2([0, 1])$ inside $\mathcal{S}_{j,p}$ such that, for any $\lambda \in \Lambda_{j,p}$, there exists some $\hat{x} = (\hat{x}_1, \hat{x}_2) \in \mathcal{Q}_{j,p} \cap \text{supp}(\psi_\lambda) \cap \partial B$ satisfying $E'(\hat{x}_1) = 0$.

Case 2b deserves a closer look. Here, we assume that for *any* $\lambda \in \Lambda_{j,p}$, there exists some $\hat{x} = (\hat{x}_1, \hat{x}_2) \in \mathcal{Q}_{j,p} \cap \text{supp}(\psi_\lambda) \cap \partial B$ satisfying $E'(\hat{x}_1) = 0$. It seems that we would need to assume that *there exists* some $\lambda \in \Lambda_{j,p}$ and some $\hat{x} = (\hat{x}_1, \hat{x}_2) \in \mathcal{Q}_{j,p} \cap \text{supp}(\psi_\lambda) \cap \partial B$ satisfying $E'(\hat{x}_1) = 0$. However, all other indices $\lambda \in \Lambda_{j,p}$ can be treated as belonging to Case 2a. Therefore, WLOG we can assume that the edge curve is a horizontal line inside $\mathcal{S}_{j,p}$, and hence *any* shearlet intersects the edge curve in some point \hat{x} with $E'(\hat{x}_1) = 0$.



FIG. 2.1. (a) A part of the curve ∂B satisfying Case 2a. Several shearlets ψ_λ , $\lambda \in \Lambda_{j,p}$, are indicated with associated feasible points $\hat{x} \in \mathcal{Q}_{j,p} \cap \text{supp}(\psi_\lambda) \cap \partial B$ satisfying $|E'(\hat{x}_2)| < \infty$. (b) A part of the curve ∂B satisfying Case 2b. Several shearlets ψ_λ , $\lambda \in \Lambda_{j,p}$, are indicated with associated feasible points $\hat{x} \in \mathcal{Q}_{j,p} \cap \text{supp}(\psi_\lambda) \cap \partial B$ satisfying $E'(\hat{x}_1) = 0$.

For both cases, we now derive estimates on the absolute value of the associated shearlet coefficients. The proofs of both propositions are contained in Section 4.

In Case 2a, the following estimate can be derived. Notice that this estimate depends on the difference in slope between the analyzing shearlet and the tangent along the curve at \hat{x} . Here the power of shearlets comes into play, which allows us to modify the shear parameter of the shearlet in order to position it on the tangent of the curve. Further, we remark that the hypothesis on ψ is implied by condition (i) (for $\ell = 0$) and condition (ii) (for $\ell = 1$) of Theorem 1.3.

PROPOSITION 2.2. *Let $\psi \in L^2(\mathbb{R}^2)$ be compactly supported and satisfy*

$$\left| \frac{\partial^\ell}{\partial \xi_2^\ell} \hat{\psi}(\xi) \right| \leq |h(\xi_1)| \cdot \left(1 + \frac{|\xi_2|}{|\xi_1|} \right)^{-\gamma}, \quad (2.2)$$

where $\gamma \geq 4$, $h \in L^1(\mathbb{R})$ and $\ell = 0, 1$. For $j \geq 0$ and $p \in \mathbb{Z}^2$, assume that $\mathcal{Q}_{j,p}$ satisfies Case 2a. Hence, for any $\lambda \in \Lambda_{j,p}$, there exists some $\hat{x} = (\hat{x}_1, \hat{x}_2) \in \mathcal{Q}_{j,p} \cap \text{supp}(\psi_\lambda) \cap \partial B$ satisfying $E'(\hat{x}_2) = s \cdot 2^{-j/2}$ for some $s \in \mathbb{R}$. Then, for all $f \in \mathcal{E}^2(\nu)$, there exists some $C > 0$ such that

$$|\langle f, \psi_\lambda \rangle| \leq C \cdot \left(\frac{2^{-3j/4}}{|k-s|^3} + \frac{2^{-7j/4}}{|k-s|^2} \right).$$

In Case 2b, we derive the following estimate. The smoothness of $\hat{\psi}$ follows from the compact support condition, and the moment condition follows from condition (i) in Theorem 1.3. Let us briefly think about this: Letting ξ_2 be fixed, condition (i)

immediately implies $\hat{\psi}(0, \xi_2) = 0$. Then, by applying Taylor expansion, it follows that $\hat{\psi}(\xi_1, \xi_2) = \frac{\partial \hat{\psi}}{\partial \xi_1}(0, \xi_2) \cdot \xi_1 + \mathcal{O}(\xi_1^2)$, and, again by condition (i), we have $\frac{\hat{\psi}(\xi_1, \xi_2)}{\xi_1} \rightarrow 0$ as $\xi_1 \rightarrow 0$, hence $\frac{\partial \hat{\psi}}{\partial \xi_1}(0, \xi_2) = 0$. This procedure can now be continued.

PROPOSITION 2.3. *Let $\psi \in L^2(\mathbb{R}^2)$ be compactly supported and satisfy*

$$\int_{\mathbb{R}} x_1^\ell \cdot \psi(x_1, x_2) dx_1 = 0 \quad \text{for all } x_2 \in \mathbb{R} \text{ and } \ell = 0, 1. \quad (2.3)$$

For $j \geq 0$ and $p \in \mathbb{Z}^2$, assume that $\mathcal{Q}_{j,p}$ satisfies Case 2b. Hence, for any $\lambda \in \Lambda_{j,p}$, there exists some $\hat{x} = (\hat{x}_1, \hat{x}_2) \in \mathcal{Q}_{j,p} \cap \text{supp}(\psi_\lambda) \cap \partial B$ satisfying $E'(\hat{x}_2) = 0$. Then, for all $f \in \mathcal{E}^2(\nu)$, there exists some $C > 0$ such that

$$|\langle f, \psi_\lambda \rangle| \leq C \cdot 2^{-11j/4}.$$

2.3. Proof of Theorem 1.3. Let $f \in \mathcal{E}^2(\nu)$. We first observe that, by Proposition 2.1, we can neglect those shearlet coefficients whose spatial support of the associated shearlet does not intersect the discontinuity curve.

To estimate the remaining shearlet coefficients, we need to analyze their decay properties. For this, let $j \geq 0$ be sufficiently large and let $p \in \mathbb{Z}^2$, be such that the associated cube satisfies $\mathcal{Q}_{j,p} \in \mathcal{Q}_j$. We note that all sets $\text{supp}(\psi_\lambda)$ with $\lambda \in \Lambda_{j,p}$ are completely included in $\mathcal{S}_{j,p}$. Therefore weights as in [1] and [11] are not required here.

We will now deal with Case 2a and Case 2b separately.

Case 2a. Let the edge curve ∂B can be parameterized by $(E(x_2), x_2)$ with $E \in C^2([0, 1])$ inside $\mathcal{S}_{j,p}$ such that, for any $\lambda \in \Lambda_{j,p}$, there exists some $\hat{x} = (\hat{x}_1, \hat{x}_2) \in \mathcal{Q}_{j,p} \cap \text{supp}(\psi_\lambda) \cap \partial B$ satisfying $E'(\hat{x}_2) = s \cdot 2^{-j/2}$ for some $s \in \mathbb{R}$.

We first show that WLOG the slope s can be replaced by a universal constant valid for any $\lambda \in \Lambda_{j,p}$. For this, consider two distinct points (\hat{x}_1, \hat{x}_2) and (\hat{y}_1, \hat{y}_2) in $\mathcal{S}_{j,p}$ such that $E'(\hat{x}_2) = s \cdot 2^{-j/2}$ and $E'(\hat{y}_2) = \hat{s} \cdot 2^{-j/2}$ with $s \neq \hat{s}$. Since $E \in C^2([0, 1])$ and – as already mentioned before – $\mathcal{S}_{j,p}$ is contained in a cubic window of size $C \cdot 2^{-j/2}$ by $C \cdot 2^{-j/2}$, we obtain $|s - \hat{s}| \leq C$. Thus $|s - \hat{s}|$ is independent on j so that we can replace the slopes by a uniform constant which for simplicity we also denote by s . Hence, we now assume that any $\lambda \in \Lambda_{j,p}$, there exists some $\hat{x} = (\hat{x}_1, \hat{x}_2) \in \mathcal{Q}_{j,p} \cap \text{supp}(\psi_\lambda) \cap \partial B$ satisfying $E'(\hat{x}_2) = s \cdot 2^{-j/2}$ for some $s \in \mathbb{R}$ independent on λ .

Letting $\varepsilon > 0$, our goal will now be to estimate first $|\Lambda_{j,p}(\varepsilon)|$ and then $|\Lambda(\varepsilon)|$. WLOG we might assume $\|\psi\|_1 \leq 1$, which implies

$$|\langle f, \psi_\lambda \rangle| \leq 2^{-3j/4}.$$

Hence, for estimating $|\Lambda_{j,p}(\varepsilon)|$, it is sufficient to restrict our attention to scales $j \leq \frac{4}{3} \log_2(\varepsilon^{-1})$.

We now consider two different cases dependent on the range of values for the slope $E'(\hat{x}_2) = s \cdot 2^{-j/2}$. The situation that the slope of the edge curve is sufficiently large so that $s \geq C \cdot 2^j$ for some constant C will be studied in the second subcase we analyze below. The first subcase handles the situation that the slope of the edge curve satisfies $s \leq C \cdot 2^j$.

Subcase $\frac{2^{-3j/4}}{|k-s|^3} \geq \frac{2^{-7j/4}}{|k-s|^2}$. In this case, by Proposition 2.2, $|\langle f, \psi_\lambda \rangle| > \varepsilon$ implies

$$|k - s| \leq C \cdot \varepsilon^{-1/3} \cdot 2^{-j/4}.$$

Observing that, for each shear index k ,

$$|\{\lambda = (j, k, m) : \lambda \in \Lambda_{j,p}\}| \leq C \cdot (|k - s| + 1),$$

we conclude

$$|\Lambda_{j,p}(\varepsilon)| \leq C \cdot \sum_{k \in K_j(\varepsilon)} (|k - s| + 1) \leq C \cdot \varepsilon^{-2/3} \cdot 2^{-j/2}, \quad (2.4)$$

where $K_j(\varepsilon) = \{k \in \mathbb{Z} : |k - s| \leq C \cdot \varepsilon^{-1/3} \cdot 2^{-j/4}\}$.

Subcase $\frac{2^{-3j/4}}{|k-s|^3} < \frac{2^{-7j/4}}{|k-s|^2}$. In this case, again by Proposition 2.2, $|\langle f, \psi_\lambda \rangle| > \varepsilon$ implies

$$|k - s| \leq C \cdot \varepsilon^{-1/2} \cdot 2^{-7j/8}.$$

We now split this subcase into two cases (coined ‘subsubcases’) dependent on the behavior of this estimate with respect to $2^{j/2}$, which becomes important due to the existence of some constant C such that

$$\#(\mathcal{Q}_j) \leq C \cdot 2^{j/2}. \quad (2.5)$$

Subsubcase $\varepsilon^{-1/2} \cdot 2^{-7j/8} < 2^{j/2}$. First, this implies

$$j > \frac{4}{11} \log_2(\varepsilon^{-1}). \quad (2.6)$$

Secondly, we can then estimate $|\Lambda_{j,p}(\varepsilon)|$ by

$$|\Lambda_{j,p}(\varepsilon)| \leq C \cdot \sum_{k \in K_j(\varepsilon)} (|k - s| + 1) \leq C \cdot \varepsilon^{-1} \cdot 2^{-7j/4} \leq C \cdot \varepsilon^{-1/2} \cdot 2^{-3j/8}, \quad (2.7)$$

where $K_j(\varepsilon) = \{k \in \mathbb{Z} : |k - s| \leq C \cdot \varepsilon^{-1/2} \cdot 2^{-7j/8}\}$.

Subsubcase $\varepsilon^{-1/2} \cdot 2^{-7j/8} \geq 2^{j/2}$. First,

$$j \leq \frac{4}{11} \log_2(\varepsilon^{-1}). \quad (2.8)$$

Using

$$|\Lambda_{j,p}| \leq C \cdot 2^j, \quad (2.9)$$

for some C , we then derive the following coarse estimate for $|\Lambda_{j,p}(\varepsilon)|$ given by

$$|\Lambda_{j,p}(\varepsilon)| \leq C \cdot 2^j, \quad (2.10)$$

which will be sufficient for our purposes.

Summarizing Case 2a, by (2.4), (2.6)–(2.10), and again (2.5),

$$|\Lambda(\varepsilon)| \leq C \cdot \left(\sum_{j=0}^{\frac{4}{3} \log_2(\varepsilon^{-1})} 2^{j/2} (\varepsilon^{-2/3} \cdot 2^{-j/2}) + \sum_{j=\frac{4}{11} \log_2(\varepsilon^{-1})}^{\frac{4}{3} \log_2(\varepsilon^{-1})} 2^{j/2} (\varepsilon^{-1/2} \cdot 2^{-3j/8}) + \sum_{j=0}^{\frac{4}{11} \log_2(\varepsilon^{-1})} 2^{j/2} \cdot 2^j \right) \quad (2.11)$$

$$\leq C \cdot \varepsilon^{-2/3} \cdot \log_2(\varepsilon^{-1}). \quad (2.12)$$

Having estimated $|\Lambda(\varepsilon)|$, we are now ready to prove our claim. Set $N = |\Lambda(\varepsilon)|$, i.e., the total number of shearlets ψ_λ such that the magnitude of the corresponding shearlet coefficient $\langle f, \psi_\lambda \rangle$ is larger than ε . By (2.11), the value ε can be written as a function of the total number of coefficients N :

$$\varepsilon(N) \leq C \cdot N^{-3/2} \cdot (\log N)^{3/2}, \quad \text{for sufficiently large } N > 0.$$

This implies that

$$|\theta(f)|_N \leq C \cdot N^{-3/2} \cdot (\log N)^{3/2}.$$

Hence,

$$\sum_{n>N} |\theta(f)|_n^2 \leq C \cdot N^{-2} \cdot (\log N)^3 \quad \text{for sufficiently large } N > 0,$$

which proves (2.1).

Case 2b. Let the edge curve ∂B can be parameterized by $(x_1, E(x_1))$ with $E \in C^2([0, 1])$ inside $\mathcal{S}_{j,p}$ such that, for any $\lambda \in \Lambda_{j,p}$, there exists some $\hat{x} = (\hat{x}_1, \hat{x}_2) \in \mathcal{Q}_{j,p} \cap \text{supp}(\psi_\lambda) \cap \partial B$ satisfying $E'(\hat{x}_1) = 0$. Let $0 < \varepsilon < 1$. Again, we aim to estimate $|\Lambda(\varepsilon)|$.

For this, suppose that $|\langle f, \psi_\lambda \rangle| > \varepsilon$. Then, by Proposition 2.3, we have $2^{-11j/4} > \varepsilon$, and hence

$$j < \frac{4}{11} \log_2(\varepsilon^{-1}).$$

By (2.9), we can conclude that

$$|\Lambda(\varepsilon)| \leq C \cdot \sum_{j=0}^{\frac{4}{11} \log_2(\varepsilon^{-1})} 2^{j/2} \cdot 2^j \leq C \cdot \varepsilon^{-2/3}.$$

This immediately implies (2.1).

The proof of Theorem 1.3 is finished.

3. Analysis of Shearlet Coefficients Associated with the Smooth Part.

In this section, we will prove Proposition 2.1. For this, we first prove a result, which shows that, provided that the shearlet ψ satisfies certain decay conditions, even with strong weights such as $(2^{4j})_j$ the system $\Psi(c, \psi)$ forms a Bessel-like sequence for $C_0^2([0, 1]^2)$.

In the following we will use the notation $r_j \sim s_j$ for $r_j, s_j \in \mathbb{R}$, if $C_1 \cdot r_j \leq s_j \leq C_2 \cdot r_j$ with constants C_1 and C_2 independent on the scale j .

LEMMA 3.1. *Let $g \in C_0^2([0, 1]^2)$, and let $\psi \in L^2(\mathbb{R}^2)$ satisfy*

$$|\hat{\psi}(\xi)| \leq C_1 \cdot \min(1, |\xi_1|^\alpha) \cdot \min(1, |\xi_1|^{-\gamma}) \cdot \min(1, |\xi_2|^{-\gamma}) \quad \text{for all } \xi = (\xi_1, \xi_2) \in \mathbb{R}^2,$$

where $\gamma > 3$, $\alpha > \gamma + 2$, and C_1 is some constant. Then, there exists some $C > 0$ such that

$$\sum_{j=0}^{\infty} \sum_{|k| \leq \lfloor 2^{j/2} \rfloor} \sum_{m \in \mathbb{Z}^2} 2^{4j} |\langle g, \psi_{j,k,m} \rangle|^2 \leq C \cdot \left\| \frac{\partial^2}{\partial x_1^2} g \right\|_2^2.$$

The proof of this lemma will explore the following result from [12], which we state here for the convenience of the reader.

PROPOSITION 3.2. [12] Let $\eta \in L^2(\mathbb{R}^2)$, and let $\psi \in L^2(\mathbb{R}^2)$ satisfy

$$|\hat{\psi}(\xi)| \leq C_1 \cdot \min(1, |\xi_1|^\alpha) \cdot \min(1, |\xi_1|^{-\gamma}) \cdot \min(1, |\xi_2|^{-\gamma}) \quad \text{for all } \xi = (\xi_1, \xi_2) \in \mathbb{R}^2,$$

where $\alpha > \gamma > 3$ and C_1 is some constant. Then, there exists some $C > 0$ such that

$$\sum_{j=0}^{\infty} \sum_{|k| \leq \lceil 2^{j/2} \rceil} \sum_{m \in \mathbb{Z}^2} |\langle \eta, \psi_{j,k,m} \rangle|^2 \leq C \cdot \|\eta\|_2^2.$$

Proof. (Proof of Lemma 3.1). By the assumption on ψ , the parameters α and γ can be chosen such that

$$|\hat{\psi}(\xi)| \leq C_1 \cdot \min(1, |\xi_1|^\alpha) \cdot \min(1, |\xi_1|^{-\gamma}) \cdot \min(1, |\xi_2|^{-\gamma}) \quad \text{for all } \xi = (\xi_1, \xi_2) \in \mathbb{R}^2,$$

where $\alpha > \gamma > 3$. Now, let $\gamma \in L^2(\mathbb{R}^2)$ be chosen to satisfy

$$\frac{\partial^2}{\partial x_1^2} \gamma = \psi.$$

Then a straightforward computation shows that γ satisfies the hypotheses of Proposition 3.2. Using integration by parts,

$$\left| \left\langle \frac{\partial^2}{\partial x_1^2} g, \gamma_{j,k,m} \right\rangle \right|^2 = 2^{4j} |\langle g, \psi_{j,k,m} \rangle|^2,$$

hence, by Proposition 3.2,

$$\begin{aligned} \sum_{j=0}^{\infty} \sum_{|k| \leq \lceil 2^{j/2} \rceil} \sum_{m \in \mathbb{Z}^2} 2^{4j} |\langle g, \psi_{j,k,m} \rangle|^2 &= \sum_{j=0}^{\infty} \sum_{|k| \leq \lceil 2^{j/2} \rceil} \sum_{m \in \mathbb{Z}^2} \left| \left\langle \frac{\partial^2}{\partial x_1^2} g, \gamma_{j,k,m} \right\rangle \right|^2 \\ &< C \cdot \left\| \frac{\partial^2}{\partial x_1^2} g \right\|_2^2. \end{aligned}$$

The proof is complete. \square

This now enables us to derive Proposition 2.1 as a corollary.

Proof. (Proof of Proposition 2.1). Let $N > 0$, and set

$$\tilde{\Lambda}_j = \{\lambda \in \Lambda_j : \text{supp}(\psi_\lambda) \cap \text{supp}(g) \neq \emptyset\}, \quad j > 0,$$

i.e., $\tilde{\Lambda}_j$ is the set of indices in Λ_j associated with shearlets whose support intersects the support of g . Then we have

$$N_J = \left| \bigcup_{j=0}^{J-1} \tilde{\Lambda}_j \right| \sim 2^{2J},$$

and thus, there exists a positive integer $j_0 > 0$ satisfying

$$N \sim N_{j_0} \sim 2^{2j_0}. \quad (3.1)$$

Hence, there exists some $C > 0$ such that

$$\begin{aligned} \sum_{j_0=1}^{\infty} 2^{4j_0} \sum_{n>N} |\theta(g)|_n^2 &\leq C \cdot \sum_{j_0=1}^{\infty} \sum_{j=j_0}^{\infty} \sum_{k,m} 2^{4j_0} |\langle g, \psi_{j,k,m} \rangle|^2 \\ &= C \cdot \sum_{j=1}^{\infty} \sum_{k,m} |\langle g, \psi_{j,k,m} \rangle|^2 \left(\sum_{j_0=1}^j 2^{4j_0} \right). \end{aligned}$$

By Lemma 3.1, this yields

$$\sum_{j_0=1}^{\infty} 2^{4j_0} \sum_{n>N} |\theta(g)|_n^2 \leq C \cdot \sum_{j=1}^{\infty} \sum_{k,m} 2^{4j} |\langle g, \psi_{j,k,m} \rangle|^2 < \infty.$$

We conclude from this, by again employing (3.1), that

$$\sum_{n>N} |\theta(g)|_n^2 \leq C \cdot (2^{2j_0})^{-2} \leq C \cdot N^{-2},$$

which completes the proof. \square

4. Analysis of Shearlet Coefficients Associated with the Discontinuity Curve. We note that the notion \sim will be utilized with the same meaning as indicated at the beginning of Section 3.

4.1. Proof of Proposition 2.2. Let $(j, k, m) \in \Lambda_{j,p}$, and choose $\hat{x} = (\hat{x}_1, \hat{x}_2) \in \mathcal{Q}_{j,p} \cap \text{supp}(\psi_\lambda) \cap \partial B$ to satisfy $E'(\hat{x}_2) = s \cdot 2^{-j/2}$ for some $s \in \mathbb{R}$. By translation symmetry, WLOG we can assume that the edge curve satisfies $E(0) = 0$ with $(\hat{x}_1, \hat{x}_2) = (0, 0)$. Further, since condition (2.2) is independent on the translation parameter m , it does not play a role in our analysis. Hence we can choose it as fitting, which we indicate by renaming it to m_0 .

Let $f \in \mathcal{E}^2(\nu)$. By exploiting the shearing property of shearlets, we have

$$|\langle f, \psi_{j,k,m_0} \rangle| = |\langle D_{S_{-s_j}} f, \psi_{j,k-s,m_0} \rangle|,$$

where $s_j = s \cdot 2^{-j/2}$. This forces the tangent to the edge curve for $D_{S_{-s_j}} f$ to have slope 0 at the origin. Hence, we can assume that $E(0) = 0$ and $E'(0) = 0$ with $k - s$ being the new shear index. From now on, we assume that $k - s \geq 0$, and set $\hat{k} = k - s$. The case $k - s < 0$ can be handled similarly.

We now consider the smallest parallelogram \mathcal{P} in the support of the shearlet ψ_{j,\hat{k},m_0} , which entirely contains the discontinuity curve $x_1 = E(x_2)$ (see Figure 4.1). Letting d be the length of one of vertical sides of \mathcal{P} , we have $2^{-j}/d \sim \hat{k}/2^{j/2}$, hence

$$d \sim \frac{2^{-j/2}}{\hat{k}}.$$

On the other hand, the horizontal diameter of \mathcal{P} is at most $C \cdot d^2$, where C only depends on smoothness of the curve $x_1 = E(x_2)$. Therefore, the volume of \mathcal{P} satisfies

$$|\mathcal{P}| \leq C \cdot \frac{2^{-3j/2}}{\hat{k}^3},$$

which in turn implies

$$|\langle f, \psi_{j, \hat{k}, m_0} \rangle| \leq C \cdot 2^{3j/4} \cdot \|f\|_\infty \cdot \|\psi\|_\infty \cdot \frac{2^{-3j/2}}{\hat{k}^3} \leq C' \cdot \hat{k}^{-3} \cdot 2^{-3j/4}.$$

Hence, WLOG the curve E can be replaced by the line $x_1 = 0$. Summarizing, it suffices to estimate $\langle f, \psi_{j, \hat{k}, m_0} \rangle$, where

$$f = f_0 \chi_\Omega, \quad \Omega = \{(x_1, x_2) \in \mathbb{R}^2 : x_1 > 0\}, \quad \text{and} \quad f_0 \in C_0^2([0, 1]^2),$$

with $\sum_{|\alpha| \leq 2} \|D^\alpha f_0\|_\infty \leq 1$. This is illustrated in Figure 4.1.

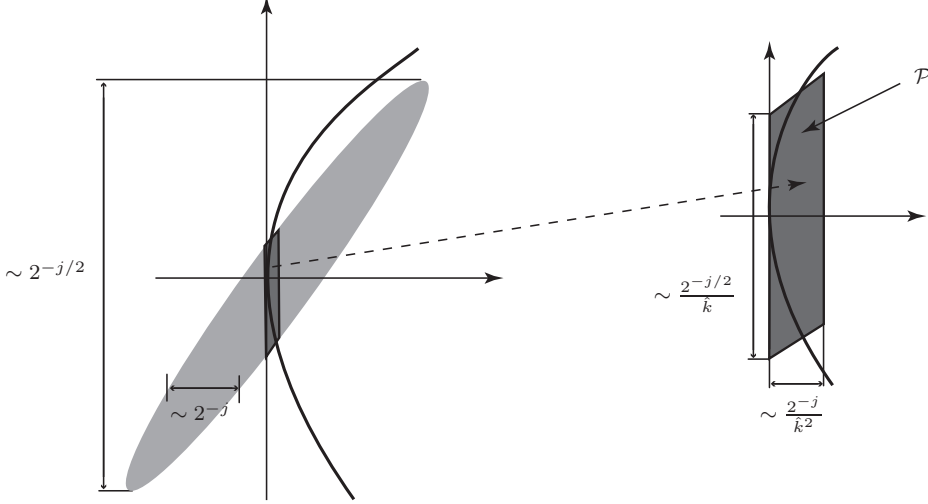


FIG. 4.1. A shearlet ψ_{j, \hat{k}, m_0} intersecting the edge curve $x_1 = E(x_2)$ with m_0 chosen close to the origin. The right hand side shows a magnification of the parallelogram \mathcal{P} .

Now, again by translation symmetry, we may assume that $\partial(\text{supp } \psi_{j, \hat{k}, m_0})$ intersects the origin. This implies that one side of the boundary $\partial(\text{supp } \psi_{j, \hat{k}, m_0})$ is asymptotically a part of the line

$$\mathcal{L} = \{(x_1, x_2) : x_2 = (2^{j/2}/\hat{k}) \cdot x_1\}$$

with slope $2^{j/2}/\hat{k}$, as described in Figure 4.2. Applying the Taylor expansion for f at each point lying on the line \mathcal{L} , we obtain

$$f(x_1, x_2) = a(x_1) + b(x_1) \left(x_2 - \frac{2^{j/2}}{\hat{k}} \cdot x_1 \right) + c(x_1, x_2) \left(x_2 - \frac{2^{j/2}}{\hat{k}} \cdot x_1 \right)^2,$$

where $a(x_1), b(x_1)$ and $c(x_1, x_2)$ are all bounded functions. This implies (compare also an illustration of the area of integration in Figure 4.2)

$$|\langle f, \psi_{j, \hat{k}, m_0} \rangle| = \left| \int_0^{C_1 \cdot \frac{\hat{k}}{2^j}} \int_{\frac{2^{j/2}}{\hat{k}} \cdot x_1}^{\frac{2^{j/2}}{\hat{k}} \cdot x_1 + C_2 \cdot \frac{2^{-j/2}}{\hat{k}}} f(x_1, x_2) \psi_{j, \hat{k}, m_0}(x_1, x_2) dx_2 dx_1 \right| \quad (4.1)$$

$$\leq C \cdot 2^{3j/4} \cdot \left| \int_0^{C_1 \cdot \frac{\hat{k}}{2^j}} I_1(x_1) + I_2(x_1) + I_3(x_1) dx_1 \right|, \quad (4.2)$$

where

$$\begin{aligned} I_1(x_1) &= \left| \int_0^{C_2 \cdot \frac{2^{-j/2}}{\hat{k}}} T_\beta \left(2^{-3j/4} \psi_{j, \hat{k}, m_0}(x_1, x_2) \right) dx_2 \right| \\ I_2(x_2) &= \left| \int_0^{C_2 \cdot \frac{2^{-j/2}}{\hat{k}}} x_2 \cdot T_\beta \left(2^{-3j/4} \psi_{j, \hat{k}, m_0}(x_1, x_2) \right) dx_2 \right| \\ I_3(x_2) &= \left| \int_0^{C_2 \cdot \frac{2^{-j/2}}{\hat{k}}} x_2^2 \cdot T_\beta \left(2^{-3j/4} \psi_{j, \hat{k}, m_0}(x_1, x_2) \right) dx_2 \right|, \end{aligned}$$

where T_β is the translation operator defined by $T_\beta(f) = f(\cdot - \beta)$ and $\beta \in \mathbb{R}$ is chosen to be $\beta = (0, -(2^{j/2}/\hat{k}) \cdot x_1)$.

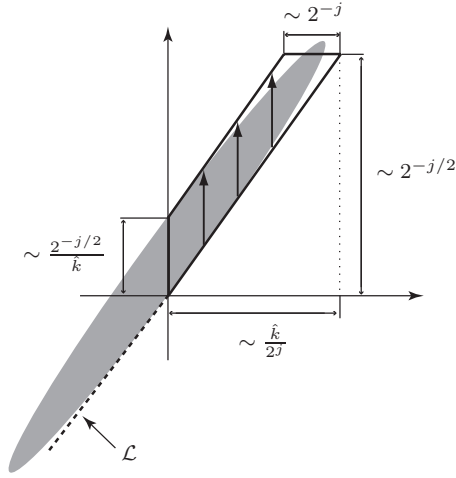


FIG. 4.2. A shearlet ψ_{j, \hat{k}, m_0} intersecting the edge curve $x_1 = 0$ with m_0 chosen such that $\text{supp}(\psi_{j, \hat{k}, m_0})$ intersects the positive x_2 axis and $\partial(\text{supp} \psi_{j, \hat{k}, m_0})$ intersects the origin. The illustration also displays the integration area for (4.1).

We first estimate $I_1(x_1)$. We observe that, since

$$\{(x_1, x_2) \in \mathbb{R}^2 : \psi_{j, \hat{k}, m_0}(x_1, x_2) \neq 0\} \subset [0, C_2 \cdot (2^{-j/2}/\hat{k})] \quad \text{for a fixed } x_1 > 0,$$

WLOG, for any $x_1 > 0$, the interval $[0, C_2 \cdot (2^{-j/2}/\hat{k})]$ for the range of the integration in $I_1(x_1)$ can be replaced by \mathbb{R} (see also Figure 4.2). Therefore, we have

$$I_1(x_1) = \left| \int_{\mathbb{R}} 2^{-3j/4} \psi_{j, \hat{k}, m_0}(x_1, x_2) dx_2 \right| = \left| \int_{\mathbb{R}} 2^{-3j/4} \hat{\psi}_{j, \hat{k}, m_0}(\xi_1, 0) \cdot e^{2\pi i \xi_1} d\xi_1 \right|. \quad (4.3)$$

Now

$$2^{-3j/4} \cdot |\hat{\psi}_{j, \hat{k}, m_0}(\xi_1, \xi_2)| = 2^{-3j/2} \cdot |\hat{\psi}(2^{-j}\xi_1, 2^{-j/2}\xi_2 + 2^{-j}\hat{k}\xi_1)|.$$

and hence, by hypothesis (2.2),

$$2^{-3j/4} \cdot |\hat{\psi}_{j, \hat{k}, m_0}(\xi_1, 0)| \leq 2^{-j/2} \cdot |2^{-j}h(2^{-j}\xi_1)| \cdot \hat{k}^{-\gamma}. \quad (4.4)$$

By (4.3) and (4.4), it follows that

$$I_1(x_1) \leq C \cdot \frac{2^{-j/2}}{\hat{k}^\gamma} \quad \text{for some } C > 0. \quad (4.5)$$

Next, we estimate $I_2(x_1)$. We have

$$\begin{aligned} I_2(x_1) &\leq \left| \int_{\mathbb{R}} 2^{-3j/4} x_2 \psi_{j,\hat{k},m_0}(x_1, x_2) dx_2 \right| + \frac{2^{j/2}}{\hat{k}} \cdot |x_1| \cdot \left| \int_{\mathbb{R}} 2^{-3j/4} \psi_{j,\hat{k},m_0}(x_1, x_2) dx_2 \right| \\ &= S_1 + S_2. \end{aligned}$$

To estimate S_1 , observe that, by (2.2),

$$\begin{aligned} S_1 &= \frac{1}{2\pi} \left| \int_{\mathbb{R}} 2^{-3j/4} \left(\frac{\partial}{\partial \xi_2} \hat{\psi}_{j,\hat{k},m_0} \right) (\xi_1, 0) e^{2\pi i \xi_1 x_1} d\xi_1 \right| \\ &\leq \frac{1}{2\pi} \int_{\mathbb{R}} (2^{-j} \cdot h(2^{-j} \xi_1)) \cdot 2^{-j} \cdot \hat{k}^{-\gamma} d\xi_1. \end{aligned} \quad (4.6)$$

By (4.5) and the fact that $0 \leq x_1 \leq C_1 \cdot \frac{\hat{k}}{2^j}$, the second term S_2 can be estimated as

$$S_2 \leq C \cdot \left(\frac{2^{j/2}}{\hat{k}} |x_1| \right) \cdot \frac{1}{2^{j/2} \cdot \hat{k}^\gamma} \leq C \cdot (C_1 2^{-j/2}) \cdot \frac{1}{2^{j/2} \cdot \hat{k}^\gamma} \leq \frac{C}{2^j \cdot \hat{k}^\gamma}. \quad (4.7)$$

Concluding from (4.6) and (4.7), we obtain

$$I_2(x_1) \leq S_1 + S_2 \leq \frac{C}{2^j \cdot \hat{k}^\gamma}. \quad (4.8)$$

Finally, we estimate $I_3(x_1)$. Notice that $2^{-3j/4} T_\beta(\psi_{j,\hat{k},m_0}(x_1, x_2))$ is bounded, hence

$$I_3(x_1) \leq C \cdot \left| \int_0^{\frac{C_2}{\hat{k} 2^{j/2}}} x_2^2 dx_2 \right| \leq \frac{C}{2^{3j/2} \cdot \hat{k}^3}. \quad (4.9)$$

Summarizing, by (4.2), (4.5), (4.8), and (4.9),

$$\begin{aligned} |\langle f, \psi_{j,\hat{k},m_0} \rangle| &\leq C \cdot 2^{3j/4} \cdot \int_0^{\frac{\hat{k}}{2^j} C_1} \left(\frac{1}{2^{j/2} \cdot \hat{k}^\gamma} + \frac{1}{2^{3j/2} \cdot \hat{k}^3} \right) dx_1 \\ &\leq C \left(\frac{1}{2^{3j/4} \cdot \hat{k}^{\gamma-1}} + \frac{1}{2^{7j/4} \cdot \hat{k}^2} \right). \end{aligned}$$

The proposition is proved.

4.2. Proof of Proposition 2.3. Applying similar arguments as in the proof of Proposition 2.2, WLOG the curve $x_2 = E(x_1)$ can be replaced by the x_1 -axis. Again, translation symmetry allows to move the center of the shearlet ψ_λ and the point \hat{x} into the origin of the spatial domain. For an illustration, we refer to Figure 4.3.

Further, we utilize that the shearing operation S_k preserves vanishing moments along the x_1 axis. This can be seen as follows. For $\ell = 0, 1$ and for a fixed $x_2 \in \mathbb{R}$, the function $x_1 \mapsto (x_1 - kx_2)^\ell$ is a polynomial of degree less than or equal to ℓ , hence, by condition (2.3) on the number of vanishing moments on ψ , we have

$$\int_{\mathbb{R}} x_1^\ell \psi(S_k(x_1, x_2))^T dx_1 = \int_{\mathbb{R}} (x_1 - kx_2)^\ell \psi(x_1, x_2) dx_1 = 0 \quad \text{for all } k \in \mathbb{R}. \quad (4.10)$$

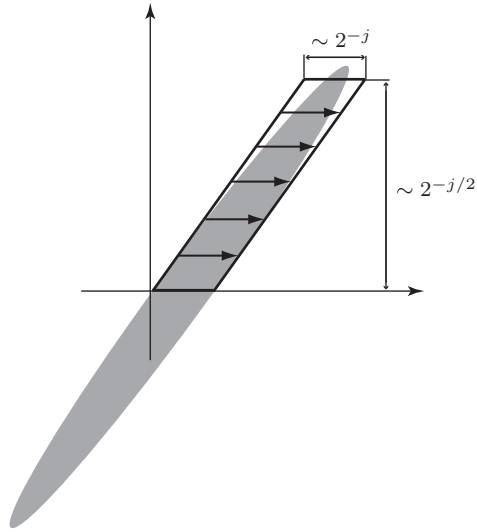


FIG. 4.3. A shearlet ψ_{j,\hat{k},m_0} intersecting the edge curve $x_2 = 0$ with m_0 chosen such that $\text{supp}(\psi_{j,\hat{k},m_0})$ intersects the positive x_1 axis and $\partial(\text{supp} \psi_{j,\hat{k},m_0})$ intersects the origin. This illustration displays the integration area for the proof of Proposition 2.3.

Employing Taylor expansion and integration (compare Figure 4.3) similar to the proof of Proposition 2.2, we finally obtain

$$|\langle f, \psi_{j,\hat{k},m_0} \rangle| \leq C \cdot 2^{3j/4} \cdot \int_0^{C_2 \cdot 2^{-j/2}} \int_0^{C_1 \cdot 2^{-j}} x_1^2 dx_1 dx_2 \leq C \cdot 2^{-11j/4},$$

and the proposition is proved.

REFERENCES

- [1] E. J. Candès and D. L. Donoho, *New tight frames of curvelets and optimal representations of objects with C^2 singularities*, Comm. Pure Appl. Math. **56** (2004), 219–266.
- [2] A. Cohen, W. Dahmen, I. Daubechies, and R. DeVore, *Tree approximation and optimal encoding*, Appl. Comput. Harmon. Anal. **11** (2001), 192–226.
- [3] S. Dahlke, G. Kutyniok, G. Steidl, and G. Teschke, *Shearlet Coorbit Spaces and associated Banach Frames*, Appl. Comput. Harmon. Anal. **27** (2009), 195–214.
- [4] M. N. Do and M. Vetterli, *The contourlet transform: an efficient directional multiresolution image representation*, IEEE Trans. Image Proc. **14** (2005), 2091–2106.
- [5] D. L. Donoho, *Wedgelets: nearly minimax estimation of edges*, Ann. Statist. **27** (1999), 859–897.
- [6] D. L. Donoho, *Sparse components of images and optimal atomic decomposition*, Constr. Approx. **17** (2001), 353–382.
- [7] D. L. Donoho and G. Kutyniok, *Microlocal Analysis of the Geometric Separation Problems*, preprint (2010).
- [8] G. Easley, D. Labate, and W. Lim, *Sparse Directional Image Representations using the Discrete Shearlet Transform*, Appl. Comput. Harmon. Anal. **25** (2008), 25–46.
- [9] K. Guo, G. Kutyniok, and D. Labate, *Sparse Multidimensional Representations using Anisotropic Dilation and Shear Operators*, Wavelets and Splines (Athens, GA, 2005), Nashboro Press, Nashville, TN (2006), 189–201.
- [10] K. Guo, D. Labate, and W. Lim, *Edge Analysis and identification using the Continuous Shearlet Transform*, Appl. Comput. Harmon. Anal. **27** (2009), 24–46.
- [11] K. Guo and D. Labate, *Optimally Sparse Multidimensional Representation using Shearlets*, SIAM J. Math. Anal. **39** (2007), 298–318.

- [12] P. Kittipoom, G. Kutyniok, and W.-Q Lim, *Construction of Compactly Supported Shearlets*, preprint (2010).
- [13] P. Kittipoom, G. Kutyniok, and W.-Q Lim, *Irregular Shearlet Frames: Geometry and Approximation Properties*, preprint (2010).
- [14] G. Kutyniok and D. Labate, *Construction of Regular and Irregular Shearlet Frames*, *J. Wavelet Theory and Appl.* **1** (2007), 1–10.
- [15] G. Kutyniok and D. Labate, *Resolution of the Wavefront Set using Continuous Shearlets*, *Trans. Amer. Math. Soc.* **361** (2009), 2719–2754.
- [16] G. Kutyniok, M. Shahrnam, and D. L. Donoho, *Development of a Digital Shearlet Transform Based on Pseudo-Polar FFT*, in *Wavelets XIII* (San Diego, CA, 2009), D. Van De Ville, V. K. Goyal und M. Papadakis, eds., 74460B-1 - 74460B-13, SPIE Proc. **7446**, SPIE, Bellingham, WA, 2009.
- [17] D. Labate, W.-Q. Lim, G. Kutyniok, and G. Weiss. *Sparse multidimensional representation using shearlets*, *Wavelets XI* (San Diego, CA, 2005), 254-262, SPIE Proc. 5914, SPIE, Bellingham, WA, 2005.
- [18] W. Lim, *Discrete Shearlet Transform: New Multiscale Directional Image Representation*, Proc. SAMPTA09, Marseille 2009.
- [19] M. Wakin, J. Romberg, C. Hyeokho, and R. Baraniuk, *Image compression using an efficient edge cartoon + texture model*, In *Data Compression Conference, 2002. Proceedings. DCC 2002*, **2-4** (2002), 43–52.

Preprint Series DFG-SPP 1324

<http://www.dfg-spp1324.de>

Reports

- [1] R. Ramlau, G. Teschke, and M. Zhariy. A Compressive Landweber Iteration for Solving Ill-Posed Inverse Problems. Preprint 1, DFG-SPP 1324, September 2008.
- [2] G. Plonka. The Easy Path Wavelet Transform: A New Adaptive Wavelet Transform for Sparse Representation of Two-dimensional Data. Preprint 2, DFG-SPP 1324, September 2008.
- [3] E. Novak and H. Woźniakowski. Optimal Order of Convergence and (In-) Tractability of Multivariate Approximation of Smooth Functions. Preprint 3, DFG-SPP 1324, October 2008.
- [4] M. Espig, L. Grasedyck, and W. Hackbusch. Black Box Low Tensor Rank Approximation Using Fibre-Crosses. Preprint 4, DFG-SPP 1324, October 2008.
- [5] T. Bonesky, S. Dahlke, P. Maass, and T. Raasch. Adaptive Wavelet Methods and Sparsity Reconstruction for Inverse Heat Conduction Problems. Preprint 5, DFG-SPP 1324, January 2009.
- [6] E. Novak and H. Woźniakowski. Approximation of Infinitely Differentiable Multivariate Functions Is Intractable. Preprint 6, DFG-SPP 1324, January 2009.
- [7] J. Ma and G. Plonka. A Review of Curvelets and Recent Applications. Preprint 7, DFG-SPP 1324, February 2009.
- [8] L. Denis, D. A. Lorenz, and D. Trede. Greedy Solution of Ill-Posed Problems: Error Bounds and Exact Inversion. Preprint 8, DFG-SPP 1324, April 2009.
- [9] U. Friedrich. A Two Parameter Generalization of Lions' Nonoverlapping Domain Decomposition Method for Linear Elliptic PDEs. Preprint 9, DFG-SPP 1324, April 2009.
- [10] K. Bredies and D. A. Lorenz. Minimization of Non-smooth, Non-convex Functionals by Iterative Thresholding. Preprint 10, DFG-SPP 1324, April 2009.
- [11] K. Bredies and D. A. Lorenz. Regularization with Non-convex Separable Constraints. Preprint 11, DFG-SPP 1324, April 2009.

- [12] M. Döhler, S. Kunis, and D. Potts. Nonequispaced Hyperbolic Cross Fast Fourier Transform. Preprint 12, DFG-SPP 1324, April 2009.
- [13] C. Bender. Dual Pricing of Multi-Exercise Options under Volume Constraints. Preprint 13, DFG-SPP 1324, April 2009.
- [14] T. Müller-Gronbach and K. Ritter. Variable Subspace Sampling and Multi-level Algorithms. Preprint 14, DFG-SPP 1324, May 2009.
- [15] G. Plonka, S. Tenorth, and A. Iske. Optimally Sparse Image Representation by the Easy Path Wavelet Transform. Preprint 15, DFG-SPP 1324, May 2009.
- [16] S. Dahlke, E. Novak, and W. Sickel. Optimal Approximation of Elliptic Problems by Linear and Nonlinear Mappings IV: Errors in L_2 and Other Norms. Preprint 16, DFG-SPP 1324, June 2009.
- [17] B. Jin, T. Khan, P. Maass, and M. Pidcock. Function Spaces and Optimal Currents in Impedance Tomography. Preprint 17, DFG-SPP 1324, June 2009.
- [18] G. Plonka and J. Ma. Curvelet-Wavelet Regularized Split Bregman Iteration for Compressed Sensing. Preprint 18, DFG-SPP 1324, June 2009.
- [19] G. Teschke and C. Borries. Accelerated Projected Steepest Descent Method for Nonlinear Inverse Problems with Sparsity Constraints. Preprint 19, DFG-SPP 1324, July 2009.
- [20] L. Grasedyck. Hierarchical Singular Value Decomposition of Tensors. Preprint 20, DFG-SPP 1324, July 2009.
- [21] D. Rudolf. Error Bounds for Computing the Expectation by Markov Chain Monte Carlo. Preprint 21, DFG-SPP 1324, July 2009.
- [22] M. Hansen and W. Sickel. Best m-term Approximation and Lizorkin-Triebel Spaces. Preprint 22, DFG-SPP 1324, August 2009.
- [23] F.J. Hickernell, T. Müller-Gronbach, B. Niu, and K. Ritter. Multi-level Monte Carlo Algorithms for Infinite-dimensional Integration on \mathbb{R}^N . Preprint 23, DFG-SPP 1324, August 2009.
- [24] S. Dereich and F. Heidenreich. A Multilevel Monte Carlo Algorithm for Lévy Driven Stochastic Differential Equations. Preprint 24, DFG-SPP 1324, August 2009.
- [25] S. Dahlke, M. Fornasier, and T. Raasch. Multilevel Preconditioning for Adaptive Sparse Optimization. Preprint 25, DFG-SPP 1324, August 2009.

- [26] S. Dereich. Multilevel Monte Carlo Algorithms for Lévy-driven SDEs with Gaussian Correction. Preprint 26, DFG-SPP 1324, August 2009.
- [27] G. Plonka, S. Tenorth, and D. Roşca. A New Hybrid Method for Image Approximation using the Easy Path Wavelet Transform. Preprint 27, DFG-SPP 1324, October 2009.
- [28] O. Koch and C. Lubich. Dynamical Low-rank Approximation of Tensors. Preprint 28, DFG-SPP 1324, November 2009.
- [29] E. Faou, V. Gradinaru, and C. Lubich. Computing Semi-classical Quantum Dynamics with Hagedorn Wavepackets. Preprint 29, DFG-SPP 1324, November 2009.
- [30] D. Conte and C. Lubich. An Error Analysis of the Multi-configuration Time-dependent Hartree Method of Quantum Dynamics. Preprint 30, DFG-SPP 1324, November 2009.
- [31] C. E. Powell and E. Ullmann. Preconditioning Stochastic Galerkin Saddle Point Problems. Preprint 31, DFG-SPP 1324, November 2009.
- [32] O. G. Ernst and E. Ullmann. Stochastic Galerkin Matrices. Preprint 32, DFG-SPP 1324, November 2009.
- [33] F. Lindner and R. L. Schilling. Weak Order for the Discretization of the Stochastic Heat Equation Driven by Impulsive Noise. Preprint 33, DFG-SPP 1324, November 2009.
- [34] L. Kämmerer and S. Kunis. On the Stability of the Hyperbolic Cross Discrete Fourier Transform. Preprint 34, DFG-SPP 1324, December 2009.
- [35] P. Cerejeiras, M. Ferreira, U. Kähler, and G. Teschke. Inversion of the noisy Radon transform on $SO(3)$ by Gabor frames and sparse recovery principles. Preprint 35, DFG-SPP 1324, January 2010.
- [36] T. Jahnke and T. Udrescu. Solving Chemical Master Equations by Adaptive Wavelet Compression. Preprint 36, DFG-SPP 1324, January 2010.
- [37] P. Kittipoom, G. Kutyniok, and W.-Q Lim. Irregular Shearlet Frames: Geometry and Approximation Properties. Preprint 37, DFG-SPP 1324, February 2010.
- [38] G. Kutyniok and W.-Q Lim. Compactly Supported Shearlets are Optimally Sparse. Preprint 38, DFG-SPP 1324, February 2010.